Numerical Weather Prediction

Notes on IASI Performance

Forecasting Research Technical Report No. 256

Andrew Collard

email: nwp_publications@metoffice.com

©Crown Copyright

Notes on IASI Performance.

by A.D. Collard.

Abstract.

The Infrared Atmospheric Sounding Interferometer (IASI) is to be launched on the METOP series of satellites starting in early 2003. IASI will be one of a new breed of infra-red atmospheric sounding instruments with high ($\lesssim 1\text{cm}^{-1}$) spectral resolution and thousands of individual channels. It is anticipated that these orders of magnitude improvement over current infra-red sounding instruments will produce large improvements in our abilities to measure atmospheric temperatures and humidities from space.

According to the mission requirements, with IASI one should be able to measure the temperature of the atmosphere with an accuracy of 1K and a vertical resolution of 1km in the lower troposphere and measure relative humidity to an accuracy of 10% and a vertical resolution of 1–2km in the same altitude range. If one interprets these requirements (as is often the case) as the ability to retrieve to the required accuracy on a grid of 1km or less, IASI retrievals will be able to reach these criteria.

Another definition of resolution is the width of the averaging kernels of the retrieval. For IASI retrievals, the averaging kernel width is 2-3km for tropospheric temperature sounding and 1-2km for humidity. These are both large improvements on the performance for HIRS-like instruments. This document also shows the relative performances of IASI and HIRS in retrieving certain interesting atmospheric temperature structures.

Notes on IASI Performance.

by A.D. Collard.

Introduction.

This document addresses three related questions concerning the Infrared Atmospheric Sounding Interferometer (IASI) instrument to be mounted on the upcoming METOP series of satellites to be launched and operated by EUMETSAT.

The IASI Mission Rationale and Requirements (MRR) document (Diebel *et al.*, 1996) states that:

> *[IASI's] measurements must be compatible in terms of sampling, resolution, accuracy and overall performances with the primary objective of providing information on:*
>
> - *the profiles of temperature in the troposphere and lower stratosphere with an accuracy of 1K, a vertical resolution of 1km in the low troposphere ... at least under cloud free conditions,*
>
> - *the profiles of water vapour in the troposphere with an accuracy of 10% on relative humidity, a vertical resolution of 1–2km in the lower troposphere ... at least under cloud free conditions ...*

The degree to which the expected performance of IASI will allow these criteria to be met is the first question to be considered in this document. The question of the exact definition of resolution is the cause of some debate. It has been suggested that the "official" IASI definition should follow that of AIRS i.e., the requirement is met if the temperature profile can be retrieved with an accuracy of 1K on a 1km grid. However, in order to highlight the great improvement in vertical resolution that IASI will provide over the current generation of instruments, this investigation will concentrate primarily on the information contained in the retrievals' averaging kernels (see next section).

A second related question is how well IASI will perform compared to current operational sounding instruments with particular reference to HIRS. One would hope that, given the large increase in spectral resolution and number of channels, IASI would be able to perform significantly better than HIRS, especially in terms of vertical resolution.

Finally, CNES has issued three possible noise performances (the minimum, typical and maximum expected noise) that IASI may eventually have to meet. The effect of degrading the noise as suggested is investigated.

The notation herein follows that recommended by Ide *et al.* (1997).

Method of Investigating Retrieval Accuracy and Vertical Resolution.

The best estimate, $\hat{\mathbf{x}}$, of the atmospheric state, $\mathbf{x}$, is in general found by minimising the cost function, $J(\mathbf{x})$, where

$$J(\mathbf{x}) = (\mathbf{x} - \mathbf{x_0})\mathbf{B^{-1}}(\mathbf{x} - \mathbf{x_0})^T + (\mathbf{y} - \mathbf{y}(\mathbf{x}))\mathbf{O^{-1}}(\mathbf{y} - \mathbf{y}(\mathbf{x}))^T \quad (1)$$

where the observations, $\mathbf{y}$, have error covariances $\mathbf{O}$; $\mathbf{B}$ is the error covariance matrix of the *a priori* measurements $\mathbf{x_0}$; and $\mathbf{y}(\mathbf{x})$ is the observed radiance that would result for a given atmospheric state $\mathbf{x}$.

For weakly non-linear problems, the approximate solution and associated error covariance

is given by the optimal estimation method of retrieval (Rodgers, 1976) where

$$\hat{\mathbf{x}} = (\mathbf{B}^{-1} + \mathbf{H}^T\mathbf{O}^{-1}\mathbf{H})^{-1}(\mathbf{B}^{-1}\mathbf{x_0} + \mathbf{H}^T\mathbf{O}^{-1}\mathbf{y}) \tag{2a}$$

and

$$\mathbf{A} = (\mathbf{B}^{-1} + \mathbf{H}^T\mathbf{O}^{-1}\mathbf{H})^{-1}. \tag{2b}$$

Here, $\mathbf{H} = \nabla_x \mathbf{y}(\mathbf{x})$ is the matrix of instrument weighting functions.

The variance of the retrieved profile is then given simply by the diagonal of $\mathbf{A}$ while information on the vertical resolution is contained in the off-diagonal terms, i.e., the inter-level correlations.

If the true atmospheric state is represented by the vector $\mathbf{x_T}$, one finds that in the linear case (e.g., Eyre (1987))

$$\begin{aligned}(\hat{\mathbf{x}} - \mathbf{x_0}) &= (\mathbf{HB})^T(\mathbf{HBH}^T + \mathbf{O})^{-1}\mathbf{H}(\mathbf{x_T} - \mathbf{x_0}) \\ &= \mathbf{R}(\mathbf{x_T} - \mathbf{x_0})\end{aligned} \tag{3a}$$

or, alternatively

$$\hat{\mathbf{x}} = \mathbf{R}\mathbf{x_T} + (\mathbf{I} - \mathbf{R})\mathbf{x_0} \tag{3b}$$

It follows that

$$\mathbf{R} = \mathbf{I} - \mathbf{AB}^{-1} \tag{4}$$

where $\mathbf{I}$ is the identity matrix.

$\mathbf{R}$ is known as either the *Averaging Kernel* (Backus and Gilbert, 1970) or the *Model Resolution Matrix* (Menke, 1984). The rows of $\mathbf{R}$ give the contributions from each level of the $\mathbf{x_T} - \mathbf{x_0}$ profile (i.e., the difference between the truth and *a priori* profiles) to a given level in the $\hat{\mathbf{x}} - \mathbf{x_0}$ profile (the difference between the retrieved and *a priori* profiles). Conversely, the columns tell one how a perturbation in a single level of $\mathbf{x_T} - \mathbf{x_0}$ is distributed over $\hat{\mathbf{x}} - \mathbf{x_0}$.

The averaging kernel can be used in a variety of ways to produce a vertical resolution for an instrument. One of the first definitions and one of the simplest is that of Backus and Gilbert (1970). Here the resolution, r_i, at level i is given by:*

$$r_i = 12\frac{\sum_j (z_i - z_j)^2 \mathbf{R}_{ij}^2/\Delta z_j}{\left(\sum_j \mathbf{R}_{ij}\right)^2} \tag{5}$$

where z_j is the height and Δz_j the height interval at level j.

A disadvantage of the Backus-Gilbert measure of spread is that it is very sensitive to negative "side-lobes" in the rows of the averaging kernel. These negative lobes cause the denominator in the RHS of Eqn. 5 to be small and thus results in a particularly large value for the resolution. A case where this occurs is shown in Figure 1, where the Backus-Gilbert vertical resolution is calculated to be 29km. This is remedied by using $|\mathbf{R}_{ji}|$ instead of $\mathbf{R}_{ji}$ in the denominator of Eqn. 5. i.e.,

$$r_i = 12\frac{\sum_j (z_i - z_j)^2 \mathbf{R}_{ij}^2/\Delta z_j}{\left(\sum_j |\mathbf{R}_{ij}|\right)^2} \tag{6}$$

* See also Appendix A.

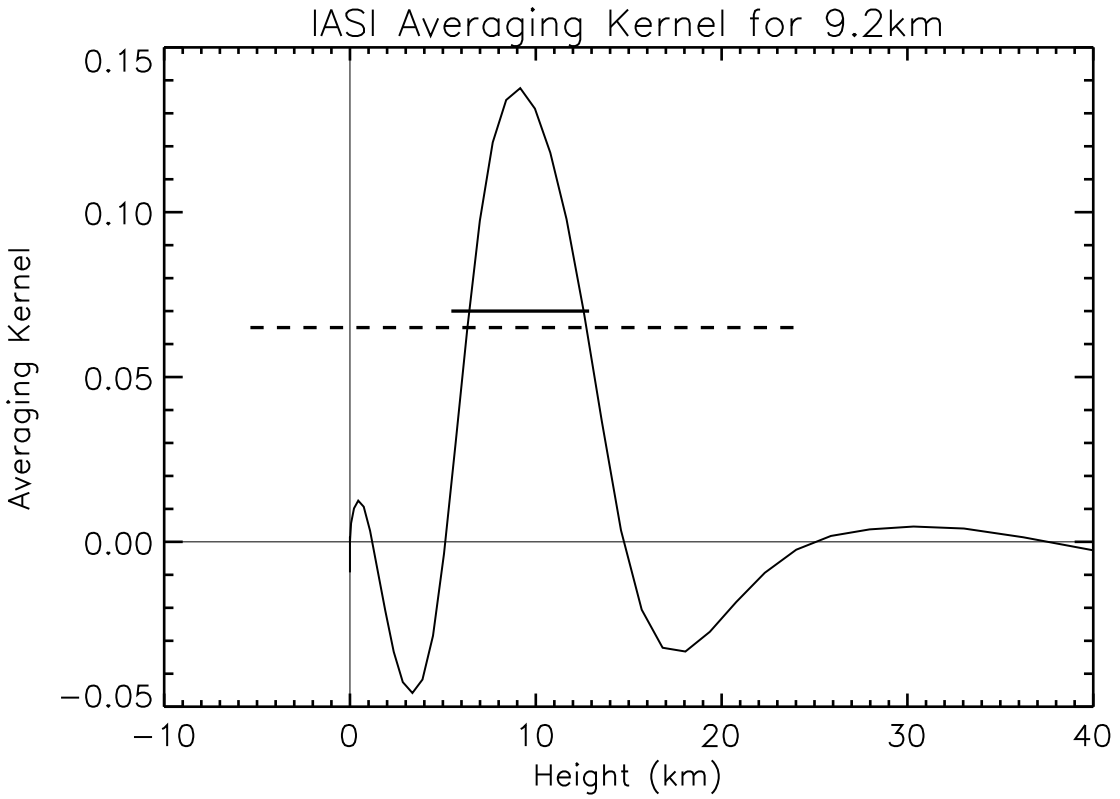

Fig. 1. The row of an IASI averaging kernel corresponding to a height of 9.2km. The averaging kernel is for a temperature only retrieval with the "maximum" noise scenario and with the 6.3μm H_2O band omitted (see text). The Backus-Gilbert resolution in this case is 29km (as indicated by the dashed horizontal line at the half-maximum level), this is reduced to 7.4km (solid horizontal line) if $|\mathbf{R}_{ji}|$ is used instead of $\mathbf{R}_{ji}$ in the denominator of Eqn. 5.

From Eqn 3b, Rodgers (1996) has shown that the number of degrees of freedom for signal (i.e., the number of separate information eigenvectors provided by the measurements) in the retrieval is given by the trace of the averaging kernel matrix, $Tr(\mathbf{R})$.

Purser and Huang (1993) use this property of the resolution matrix to define vertical resolution in terms of effective data density, ρ, where the data density, ρ_i, for layer i of thickness Δz_i is given by

$$\rho_i = R_{ii}/\Delta z_i \tag{7}$$

The vertical resolution by this definition is thus $1/\rho_i$ for level i. Purser and Huang go on to define a smoothing operator based on the correlation structure of $\mathbf{R}$ to eliminate the worst of the level-to-level fluctuations in ρ, but for the examples in this document this does not appear to be a problem and the simpler definition is preferred.

Rodgers (1990) shows that the analysis error covariance, $\mathbf{A}$, can be thought of as the sum of two error covariances, $\mathbf{A}_N$ and $\mathbf{A}_M$ corresponding to the contributions from the null-space and measurement errors respectively ($\mathbf{A}_M$ is hereinafter referred to as the "propagated measurement error"). For the optimal estimation method,

$$\mathbf{A}_N = (\mathbf{B}^{-1} + \mathbf{H}^T\mathbf{O}^{-1}\mathbf{H})^{-1}\mathbf{B}^{-1}(\mathbf{B}^{-1} + \mathbf{H}^T\mathbf{O}^{-1}\mathbf{H})^{-1} \tag{8a}$$

and

$$\mathbf{A}_M = (\mathbf{B}^{-1} + \mathbf{H}^T\mathbf{O}^{-1}\mathbf{H})^{-1}\mathbf{H}^T\mathbf{O}^{-1}\mathbf{H}(\mathbf{B}^{-1} + \mathbf{H}^T\mathbf{O}^{-1}\mathbf{H})^{-1}. \qquad (8b)$$

The null-space error arises from the fact that the retrieved profile is a smoothed version of the truth with the *a priori* profile providing those components where the observations do not add information (as shown by Eqn. 3b). Thus the analysis error covariance, $\mathbf{A} = \mathrm{E}\left[(\hat{\mathbf{x}} - \mathbf{x_t})(\hat{\mathbf{x}} - \mathbf{x_t})^T\right]$, has a component which accounts for the smoothing error.

As the error due to smoothing is already included in the analysis error covariance, one can argue that if the diagonal elements of $\mathbf{A}$ are less than $1\mathrm{K}^2$ when one is retrieving on a 1km grid, the 1km-1K criterion has been met. Alternatively, it can be argued that if one is using the spread of the averaging kernels as a definition of resolution, it is more appropriate to consider the diagonals of $\mathbf{A}_M$ rather than $\mathbf{A}$ as in the latter case one would also including the effect of resolution. Therefore, in the following both the retrieval and propagated measurement errors are shown.

From Eqns. 3a and 7b, one can show that if $\mathbf{y_T} = \mathbf{H}\mathbf{x_T}$ is the noise-free radiance that would correspond to the true atmospheric state, $\mathbf{x_T}$,

$$(\hat{\mathbf{x}} - \mathbf{x_0})^T\mathbf{A}_M^{-1}(\hat{\mathbf{x}} - \mathbf{x_0}) = (\mathbf{y_T} - \mathbf{y_0})^T\mathbf{O}^{-1}(\mathbf{y_T} - \mathbf{y_0}), \qquad (9)$$

i.e., comparing the retrieved profile to the propagated measurement noise is equivalent to comparing the observed radiance signal to the instrument noise.

Calculation of Retrieval Properties for IASI.

These investigations required the analysis covariance matrix, $\mathbf{A}$, to be calculated from *a priori* data error covariance and the measurements' error covariance using appropriate IASI weighting functions, $\mathbf{H}$. The weighting functions used were calculated for a mid-latitude winter case using the IASI fastmodel (IASIRTM) being developed by Marco Matricardi (ECMWF). The measurement error covariance matrix is assumed to be diagonal with its elements being the square of the instrument noise plus a constant forward model error of $(0.2\mathrm{K})^2$. The *a priori* covariance matrix used is the ECMWF 40-level background error covariance which has been interpolated onto the 43 levels of the Jacobians (see Appendix B).

The 43 level model has the advantage (over the previous 40-level model) of much higher vertical resolution, especially in the lower part of the atmosphere where the height interval is as low as 0.2km. Only the lowest 28 of the available levels are used in humidity retrievals, resulting in a total of 72 retrieved parameters (43 atmospheric temperatures, the skin temperature and 28 humidities).

Four instrument noises are considered; the latest "Cannes" specification and three noise curves corresponding to the minimum, typical and maximum degradations estimated by CNES. The three latter noise curves are consistent with an apodised (level 1c) spectrum, with the apodisation corresponding to an Gaussian instrument response function with a $0.5\mathrm{cm}^{-1}$full width at half maximum. This is the same apodisation that is used in the fastmodel calculations. The "Cannes" specification noise is defined for unapodised (level 1a) data and thus this noise curve is corrected using the method of Lee (priv. comm.)[1].

[1] Distributed in U.K. Met. Office (RSI) Branch Working Paper 117 which is an internal document and may not be quoted directly.

The HIRS noise values come from Table 3.2.1-2 of the NOAA KLM Users Guide which can be found on-line at `http://perigee.ncdc.noaa.gov/docs/klm/html/c3/sec3-2.htm#t321-2` to which a forward modeling error of 0.2K is added in quadrature.

Temperature Retrievals - General Case.

In this section we shall look at the expected performance of IASI retrievals of temperature. We shall look at two cases, one where all the IASI spectral channels are used and the humidities and temperatures are retrieved simultaneously (but see the discussion below on non-linearity) and one where the strong 6.3μm H_2O band is omitted* and temperature alone is retrieved.

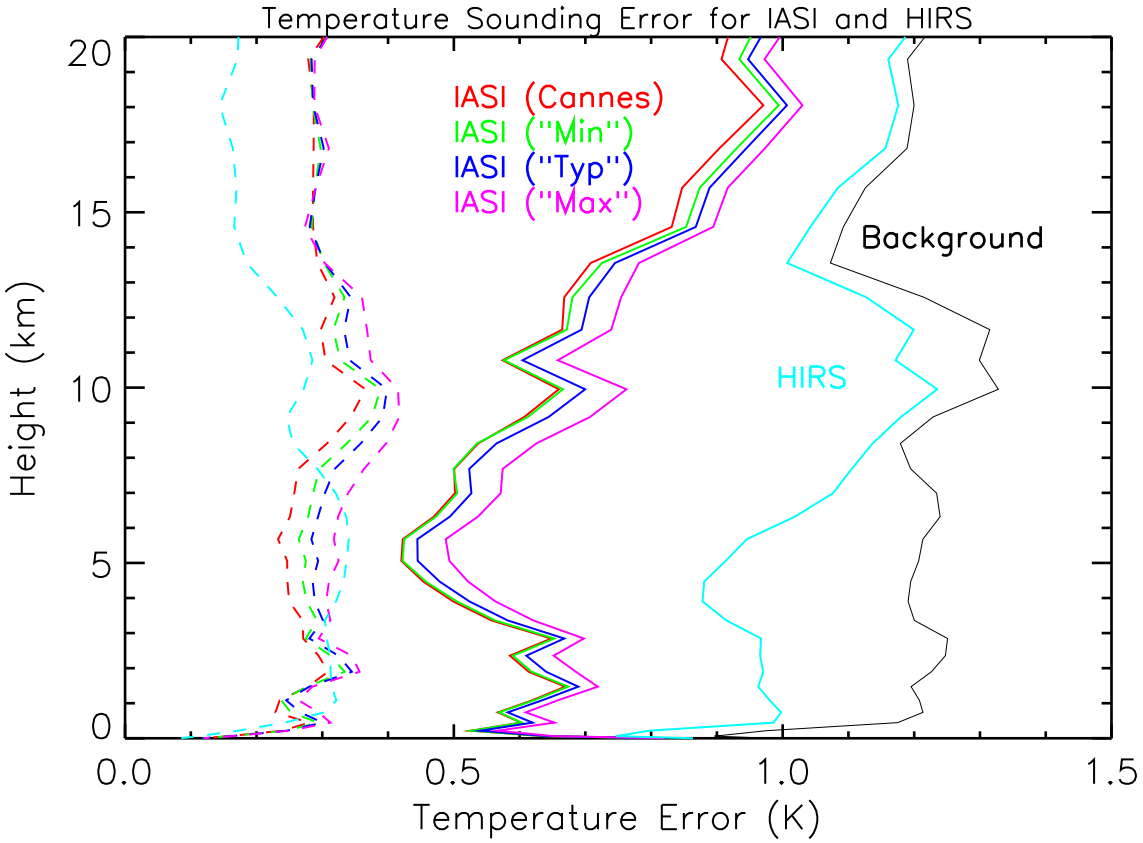

Fig. 2a. IASI and HIRS temperature retrieval noise using all channels in each instrument. The solid lines are from the analysis error covariance matrices while the dashed lines are propagated measurement noise.

As will be seen, the very sharp lines in the water band greatly improve the vertical resolution of the retrieval but, of course, one would need to have good information on the vertical profile of H_2O to take advantage of this. It is expected that the eventual retrieval scheme will involve simultaneous retrieval of humidity and temperature, in which case the actual performance will be somewhere between the two cases presented here.

The issues involved in simultaneous retrieval of temperature and humidity will be investigated in more detail at a future date when the effect of the non-linearity of the weighting

* When the H_2O band is omitted from the IASI calculations, frequencies between 1235cm^{-1} and 2170cm^{-1} are ignored. In the HIRS comparisons, channels 1-8, 10-15 are used in the all IASI channels case and 1–8, 13–15 in the case where the H_2O band is omitted.

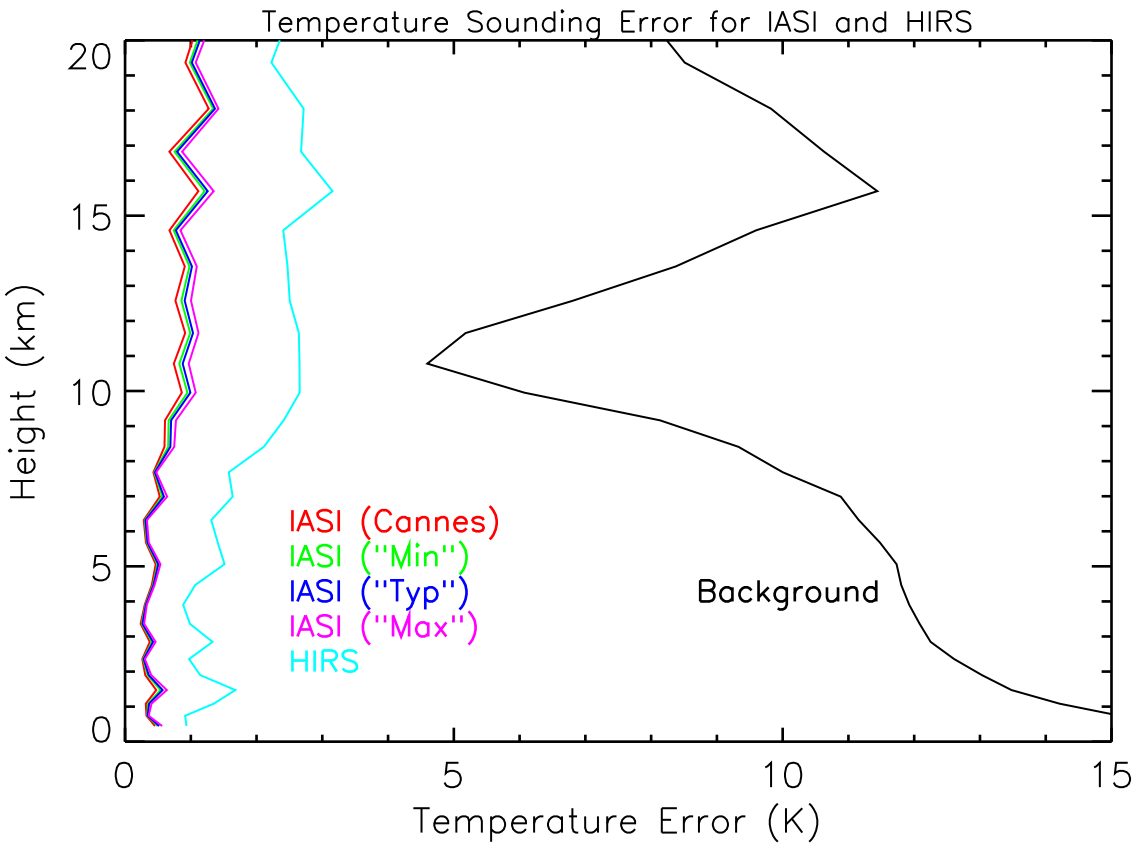

Fig. 2b. As Fig. 2a except the background error covariance now describes climatological variation rather than forecast error (see text).

functions (including the dependence on water amount of the temperature Jacobians) will be taken into account following the ideas of Eyre (1998).

Figure 2a shows the expected standard deviations (i.e., the square-root of the diagonals of the retrieved profile's error covariance matrix, $\mathbf{A}$) and the corresponding values for the propagated measurement noise (dashed lines) for the four possible IASI NEΔTs and for HIRS. It can be seen that IASI shows a clear improvement over HIRS and for much of the troposphere the retrieval noise is around 0.6K, which is much better than the performance required by the MRR. Also note that the effect of the suggested noise degradation is minimal.

While the above is a good example of the impact of IASI in the type of situation in which its data will be used, it is informative to see how it compares to HIRS when the background is less well known. Fig. 2b shows the situation when the background error variances are based on climatology. In this case the background error covariance is calculated from 1200 radiosondes and rocketsondes selected from various locations around the globe (obtained from NOAA/NESDIS). Here the retrieval error for IASI is twice as good as that for HIRS and is well below 1K throughout the lower and middle troposphere.

It is interesting to note that the retrieval performance when the climatological background error covariance matrix is used is similar to that with the forecast error covariance matrix. Clearly, IASI is doing a good job at measuring those structures in the atmosphere that have the highest climatological variability. This result would imply that the climatological error covariance matrix could also be used in obtaining a 1DVAR retrieval from IASI observations. However, given the amplitude of the variability in the climatological B matrix it is unlikely that the statistics are truly Gaussian in this case and so the assumption of linearity in Eqn. 2a is no longer valid.

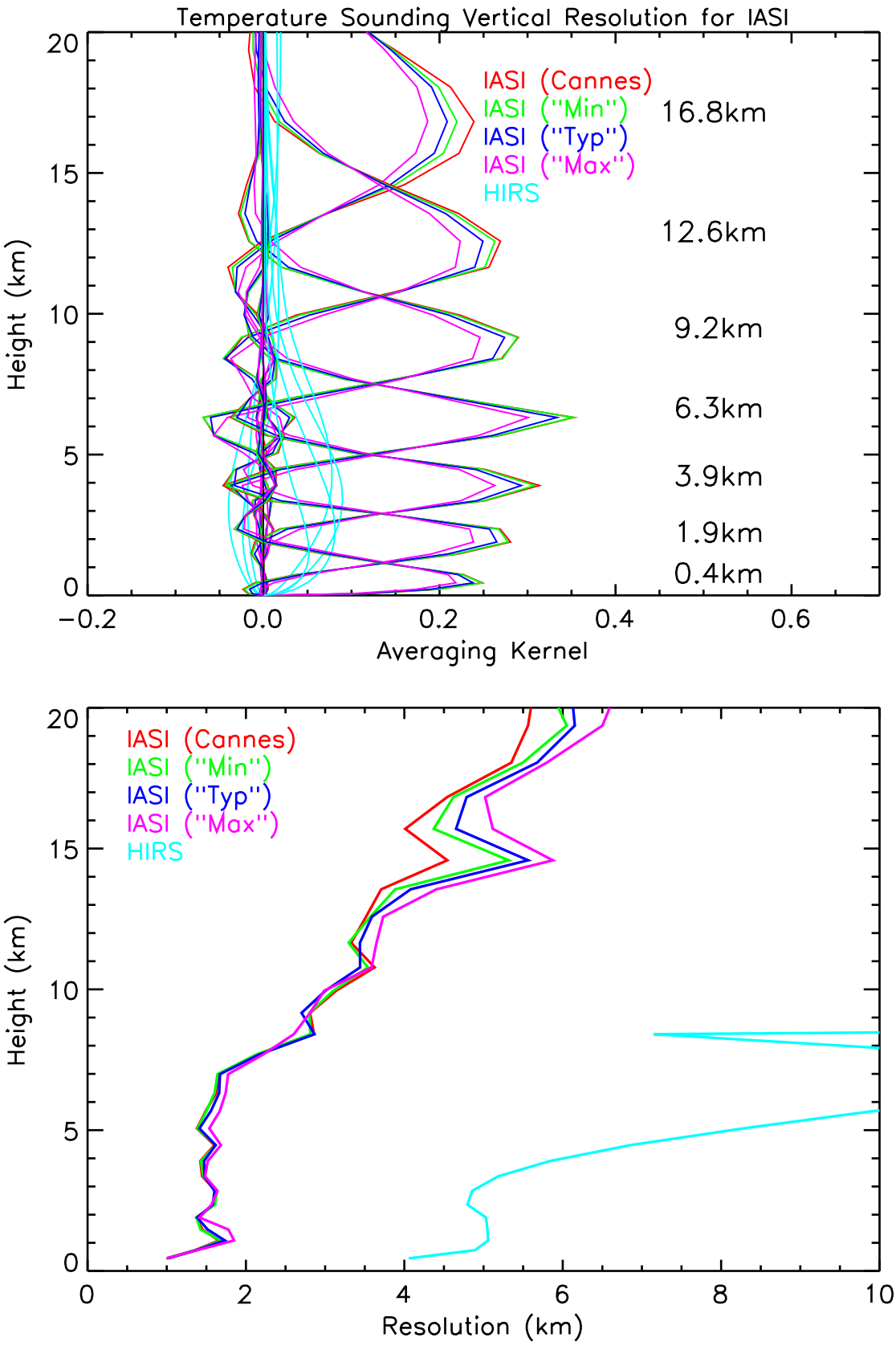

Fig. 3a. (Top) Selected averaging kernels for the retrieval of temperature using all available channels. The heights associated with each averaging kernel is indicated. Fig. 3b (Bottom) Backus-Gilbert widths of the averaging kernels above as a function of height.

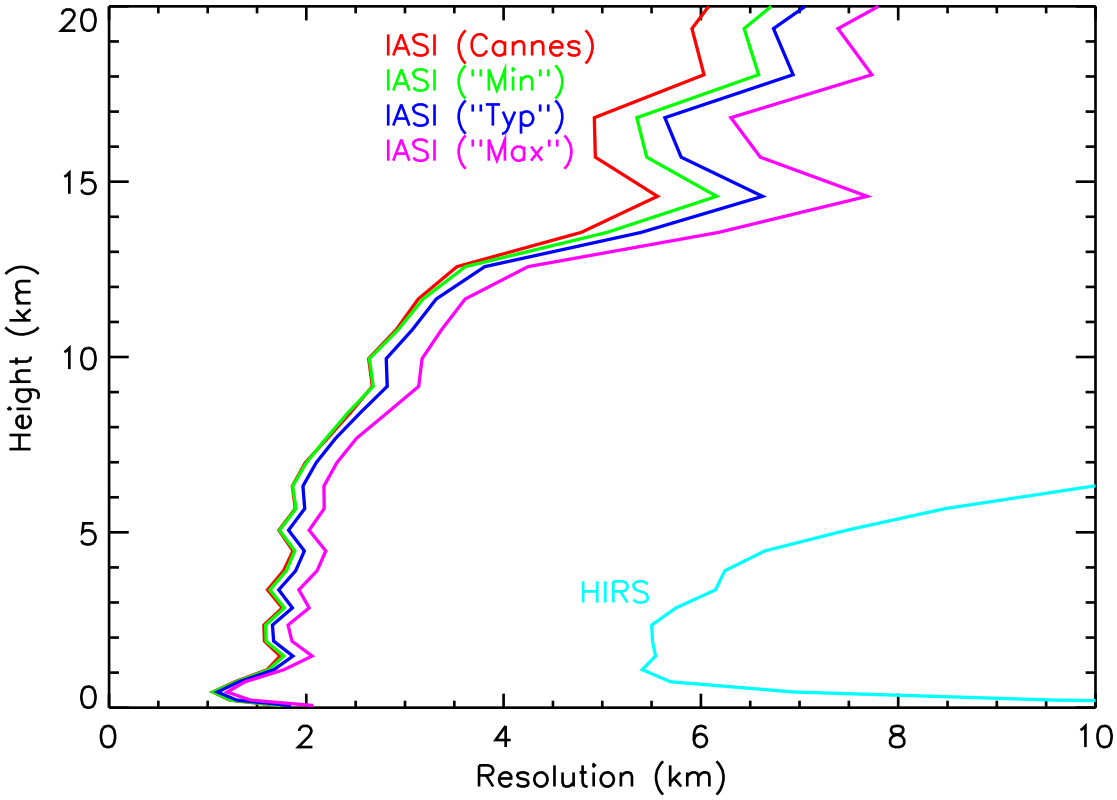

Fig. 3c. Vertical resolution of temperature retrievals defined in terms of effective data density.

The vertical spacing of the grid used in these retrievals is less than 1km throughout the troposphere and therefore the requirement of 1km-1K retrieval accuracy is easily met using the "AIRS" definition for the whole troposphere when a forecast background is used and for the lower and mid-troposphere when the *a priori* information is less well known.

Figures 3a-c show selected averaging kernels for IASI and HIRS and the vertical resolutions calculated from the **R** matrix using Eqns. 6 and 7. From these plots it can be seen that for the case where the forecast background error covariance is used:

1) IASI has much better vertical resolution than HIRS at all levels.

2) At least in the troposphere, the vertical resolution is relatively insensitive to the measurement noise level.

The number of degrees of freedom for signal, as calculated from $Tr(\mathbf{R})$, is 12.5 for the "Cannes" specification case. For the degraded noise cases this drops to 12.0, 11.4 and 10.4 for the minimum, typical and maximum noises respectively. This compares to 2.9 for HIRS. Hence there is some degradation in the number of independent pieces of information supplied by IASI on degrading the noise but this is relatively small compared to the improvement over HIRS performance. Fig. 3 also implies that the effect of the loss of these two degrees of freedom is mostly seen at stratospheric and upper tropospheric heights rather than lower down.

The case where the 6.3μm H_2O band is omitted is similar but less pronounced. Fig. 4 shows the standard deviations, and Fig. 5 the averaging kernels and the vertical resolutions in the same way as before. The situation with the temperature retrieval error is much the same

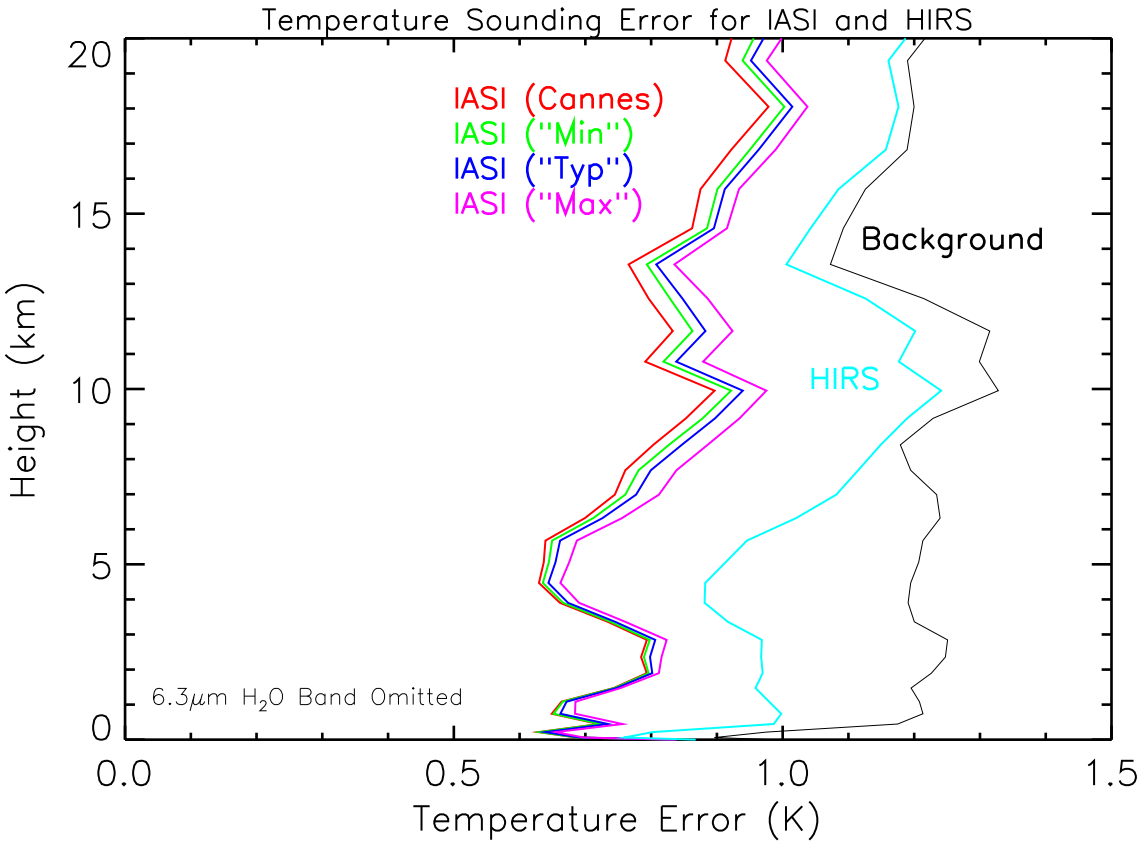

Fig. 4. As Fig. 2a except the 6.3μm H_2O band is omitted from the calculations.

as before; the IASI error is a marked improvement on HIRS throughout the troposphere although it is typically 0.7–0.8K rather than the 0.6K that was achieved when all channels were considered. The 1km-1K requirement is still met by the AIRS definition, however.

The vertical resolution of IASI in this case is also far superior to the equivalent HIRS performance. However, the sharp averaging kernels we saw in the case where all channels were used are now significantly broader. Clearly use of the sharp H_2O lines are crucial if one wants to achieve IASI's full potential with regard to vertical resolution. Incidentally, the averaging kernels for the current AIRS temperature retrieval (which uses a total of 125 channels in the 4.3μm and 15μm CO_2 bands) are of similar width to those shown in Fig. 5a (M. Goldberg, priv. comm.).

The effect of the CNES noise degradations on the retrieval error and vertical resolution in these cases are still relatively small in the lower troposphere, although there is now some degradation in the upper troposphere and, as in the previous case, at stratospheric levels. In terms of degrees of freedom for signal, the values are 9.8, 9.2, 8.8 and 8.1 for the specification and minimum, typical and maximum degradation respectively. The equivalent HIRS value is 2.8. Hence, again some information will be lost in relaxing the noise constraints on IASI but its performance in both vertical resolution and retrieval accuracy will still be far superior to the current generation of infra-red sounders.

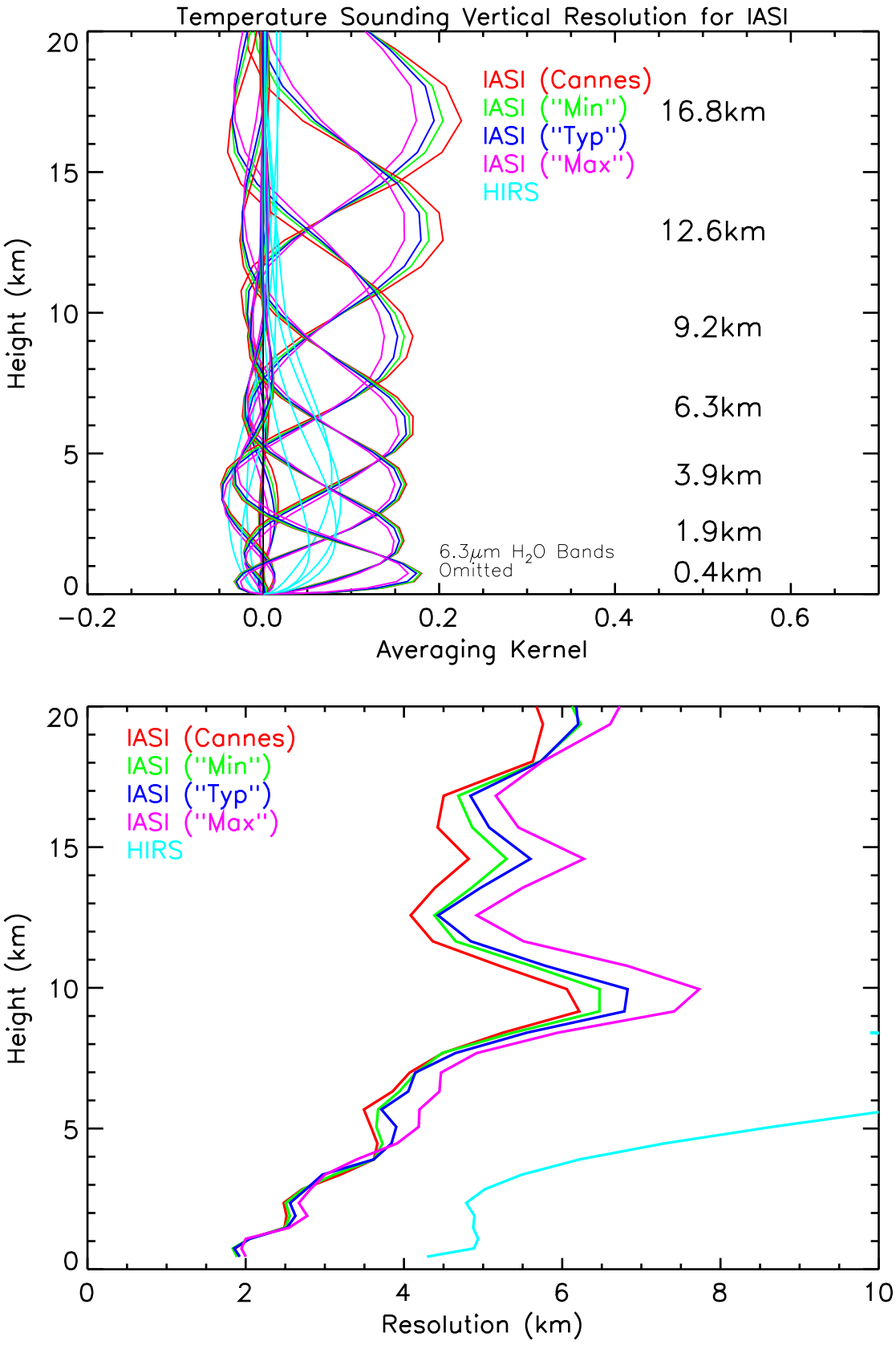

Fig. 5ab. As Fig. 3 except the 6.3μm H_2O band is omitted from the calculations.

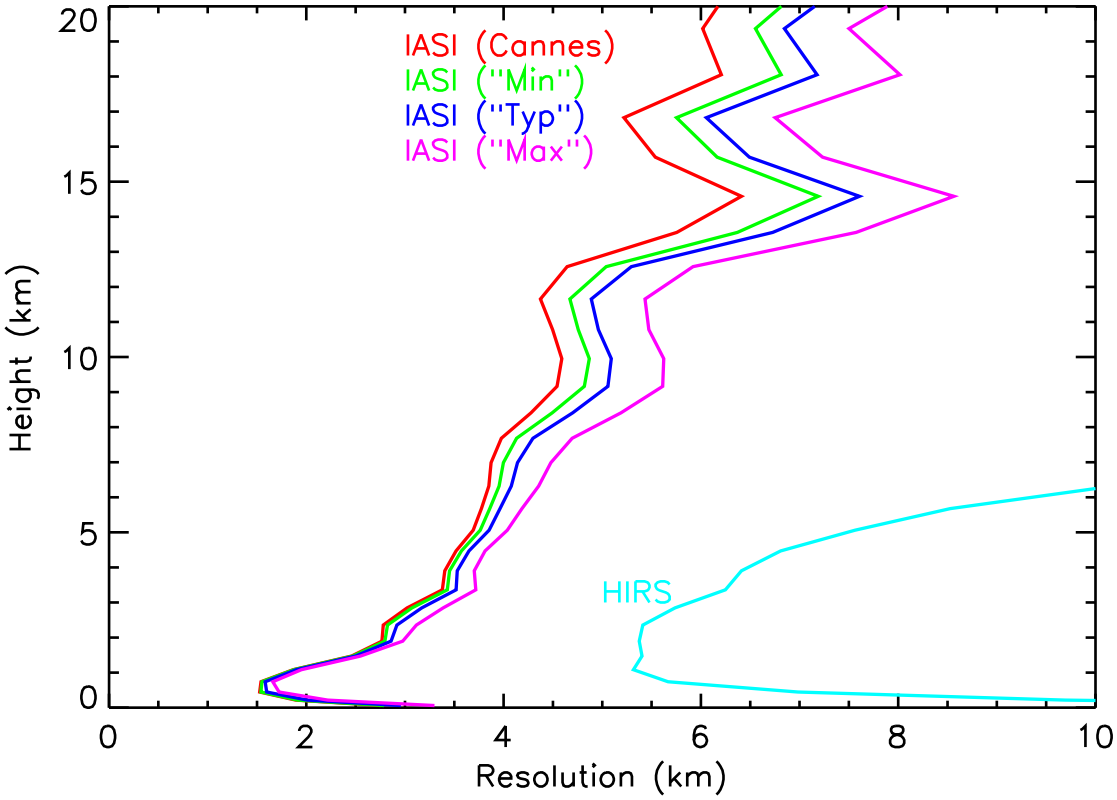

Fig. 5c. As Fig. 3c except the 6.3μm H_2O band is omitted from the calculations.

Temperature Retrievals - Specific Profiles.

Using the relationship between the true and retrieved profiles in Eqn. 3a, one can investigate the form of the profiles that would emerge from a given input temperature perturbation.

An example of this is shown in Fig. 6a where two atmospheric structures are considered that were identified by Rabier *et al.* (1996) as being important in the failed forecasting of the reintensification of the remnants of Hurricane Floyd over Brittany and SW England in September 1993. These structures were used in a previous investigation of IASI's expected performance by Prunet *et al.* (1998).

Following equation 3a, the "Rabier curves" in Fig. 6a are also plotted as they would be retrieved using either the HIRS or IASI (specification and maximum noise degradation cases) and the ECMWF forecast error covariance matrix. For both curves, the IASI retrievals reproduce the original structures well, while the HIRS retrievals are much less successful.

Fig. 6b is identical to Fig. 6a except the standard deviations from the analysis and the propagated measurement noise error covariance matrices are added to give an indication of the likely observability of the perturbations *.

As discussed earlier, the analysis error covariance includes both the error due to the prop-

* If one wants to get an exact figure on observability of a given perturbation structure one must also consider the correlation structure of the error covariance matrix and even then the interpretation depends crucially on the exact situation in which the information is to be used. This is beyond the scope of the current document.

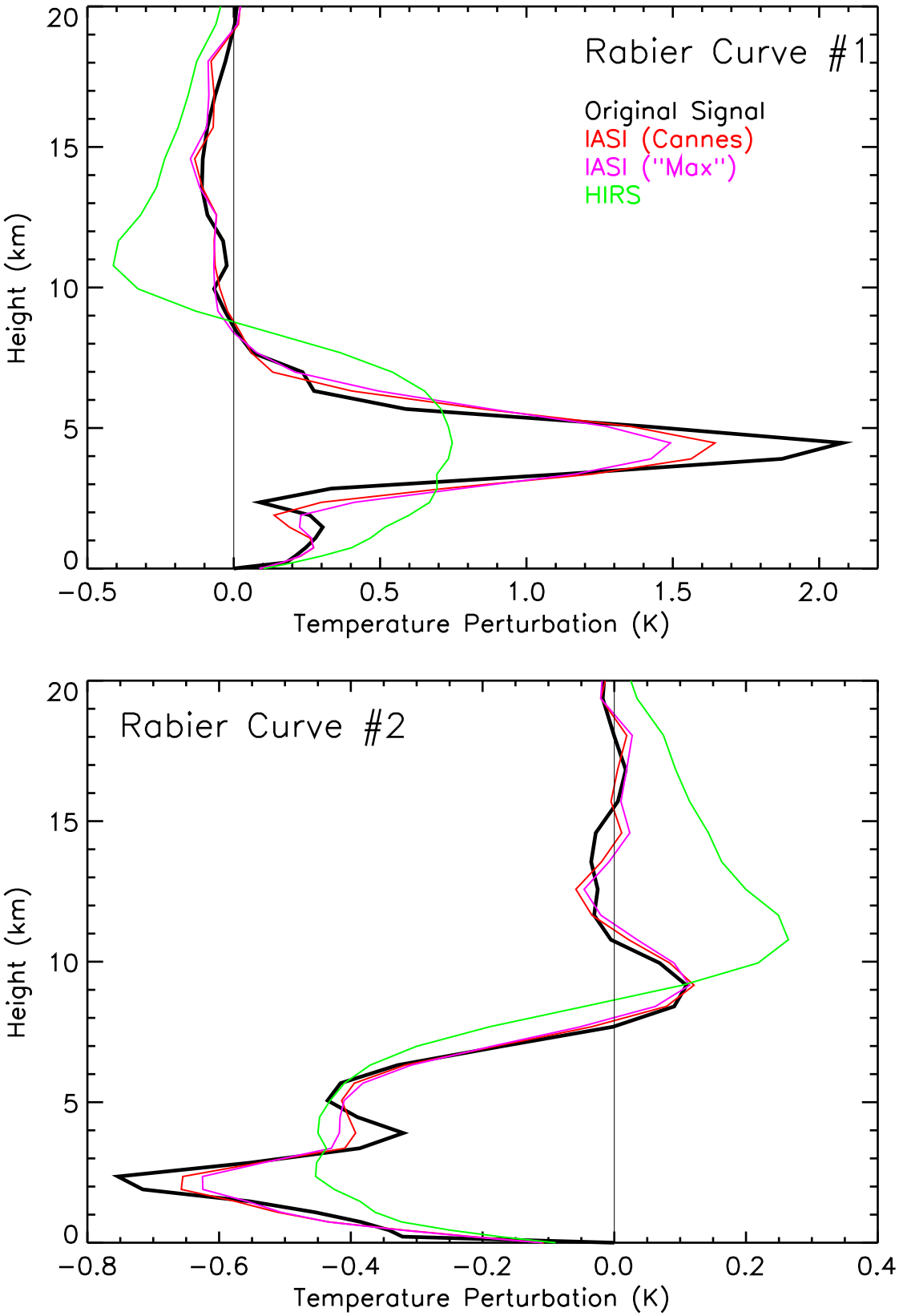

Fig. 6a. The two "Rabier curves" used by Prunet et al. and the corresponding profiles that would be retrieved by the HIRS and IASI instruments as calculated via the resolution matrix.

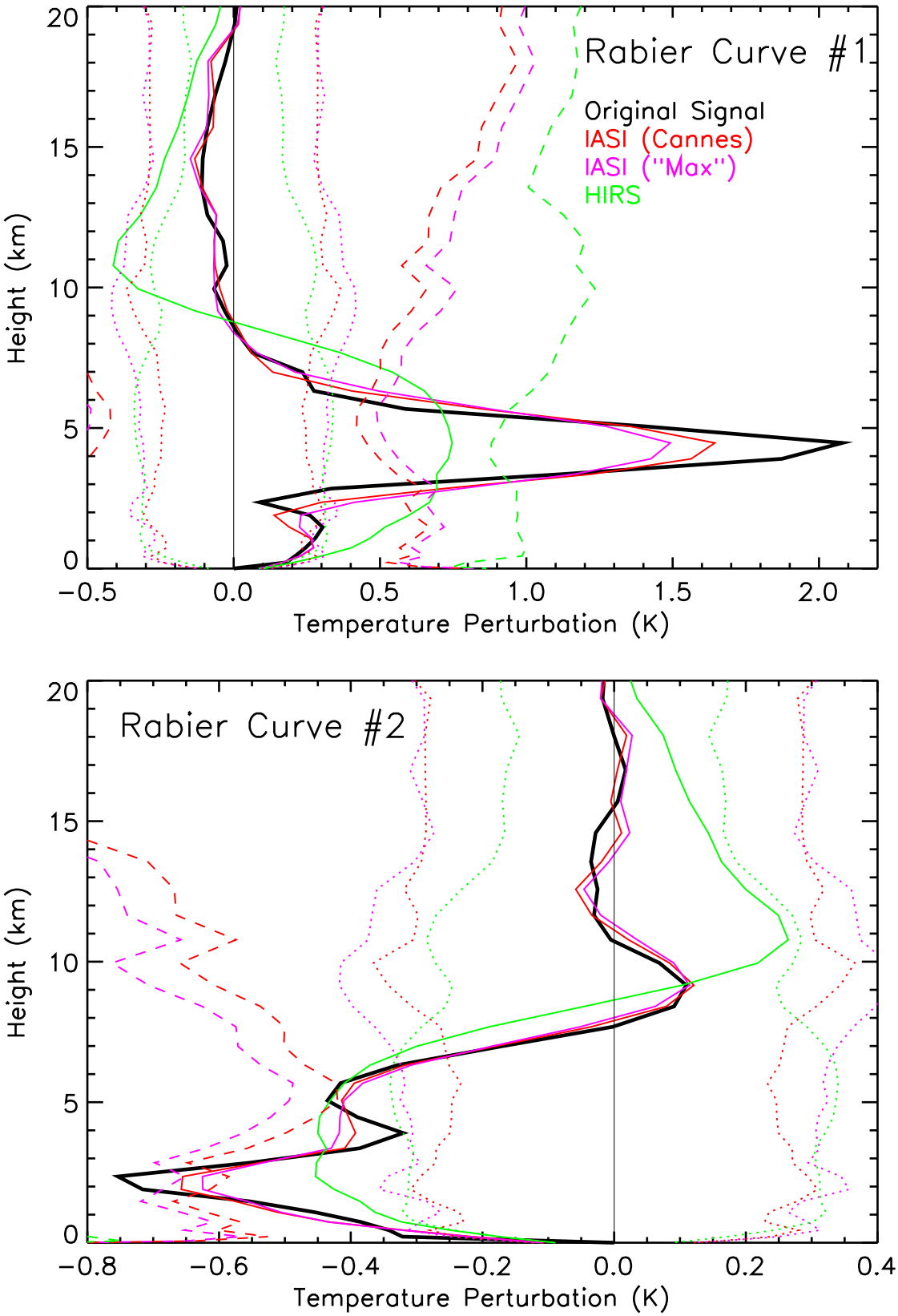

Fig. 6b. As Fig. 6a except diagonals of the analysis (dashed lines) and propagated measurement noise (dotted lines) error covariance matrices are added.

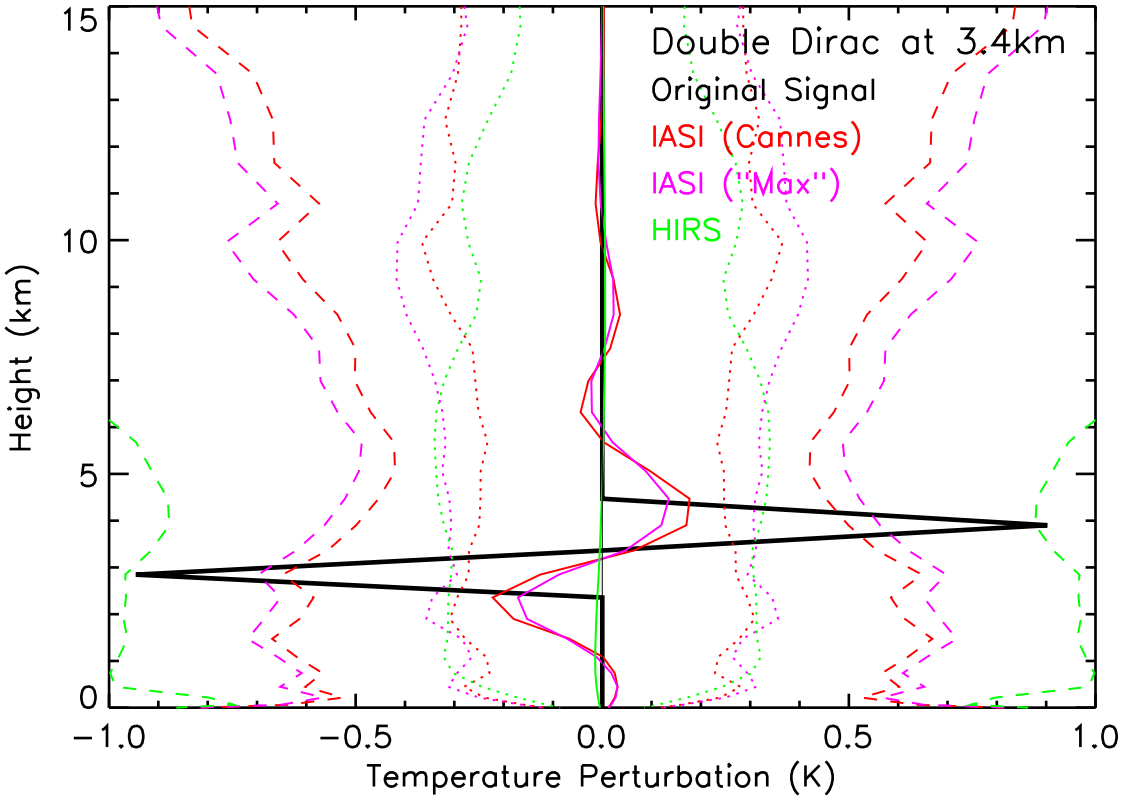

Fig. 7. As Fig. 6 except the perturbation profile is a 1km-1K "double-Dirac" function (following Lee) around the 3.4 km.

agated measurement noise and the smoothing or null-space error due to fact that certain structures cannot be measured by the observing system. The effect of the smoothing error can be plainly seen in this plot in the difference in shape between the "true" and retrieved profiles and so in this case one should compare the "retrieved" profile with the propagated measurement error when estimating the observability of the structures shown. This is supported by the relation in Eqn. 9.

In the case of the Rabier curves, one can see that the IASI retrieval signals are well above their noise levels while the corresponding HIRS retrievals have a much lower signal to noise ratio and detection of this signal would be marginal.

Fig. 7 is a similar plot to Fig. 6b except now the hypothetical "double-Dirac" perturbation of Lee (priv. comm.[1]) is used at a level that he identified as crucial in assessing IASI performance. In this case the IASI retrieval significantly smears out the perturbation while the HIRS retrieval smoothes it out entirely. Even for the IASI case, the noise levels are somewhat higher than the retrieved signal, however, and detectibility of these perturbations is thus marginal.

Humidity Retrievals.

As mentioned earlier, only the lowest 28 levels are used in humidity retrievals. The standard deviations calculated for humidity for a simultaneous retrieval are shown in Figure 8. While the retrieval errors for IASI are significantly better than for HIRS, they appear to fall short of the desired 10% on the pressure levels used. However, the requirement is for accuracy

[1] WP 117

of better than 10% in *relative* humidity and so given an average situation of 50% relative humidity, the retrieval accuracy for relative humidity will meet the requirements.

If one were to do the retrieval on a coarser 1km grid, one might get closer to 10% accuracy even in the absolute sense. However, due to the inter-level correlations it is not straightforward to infer from the current results what the retrieval errors would be if this were the case, although values of 15–20% in absolute humidity seem reasonable for the tropospheric levels.

Fig. 9a-c shows the averaging kernels and associated the Backus-Gilbert widths and effective data densities for the humidity retrieval. The averaging kernels for IASI are very sharp and for many levels it is apparent that the pressure levels being used in the retrievals are not adequate to properly represent them (motivating the production of a fastmodel with yet higher vertical resolution than the current 43 level one). However, from Figs. 9b and 9c, it is clear that the vertical resolution in this case is close to the 1km requirement.

On inspecting the trace of the **R** matrix for humidity, the number of degrees of freedom for signal are 12.6, 12.5, 11.8 and 10.4 for Cannes specification and the minimum, typical and maximum projected performances respectively. For HIRS there are 1.8 degrees of freedom.

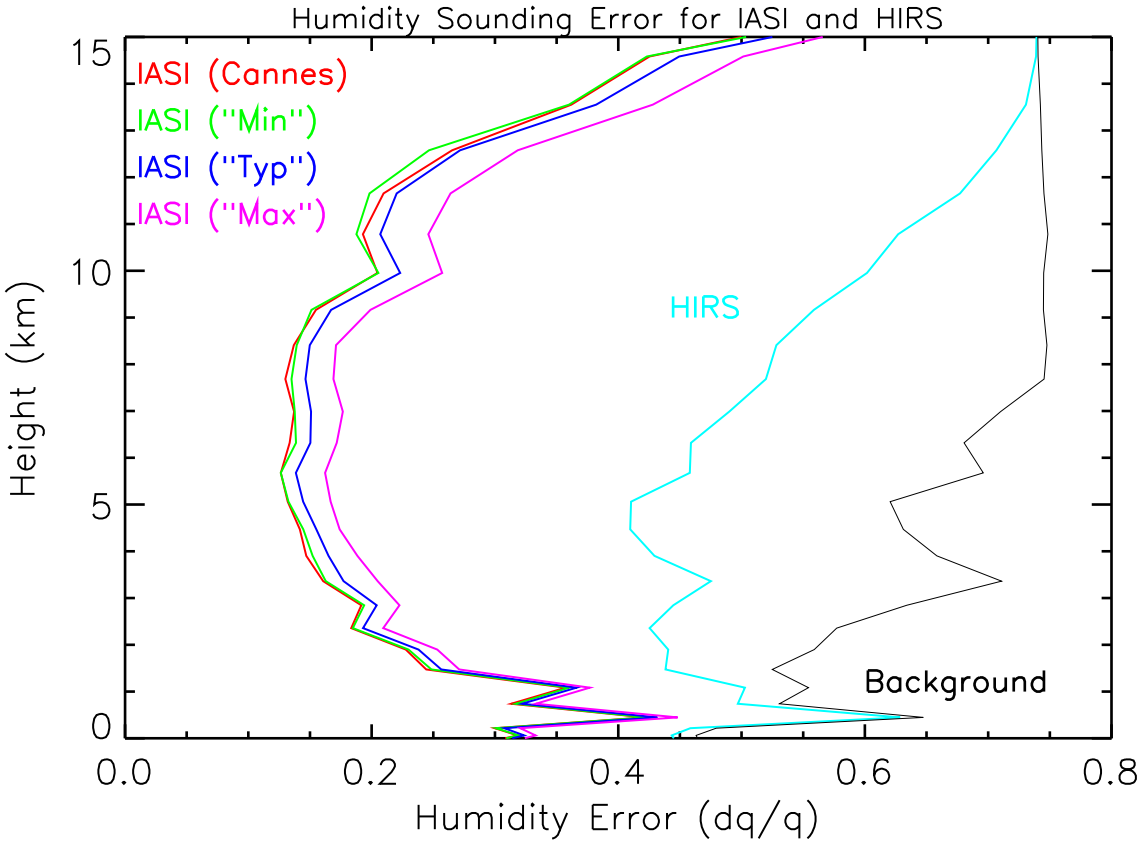

Fig. 8. IASI and HIRS humidity retrieval noise using all channels in each instrument.

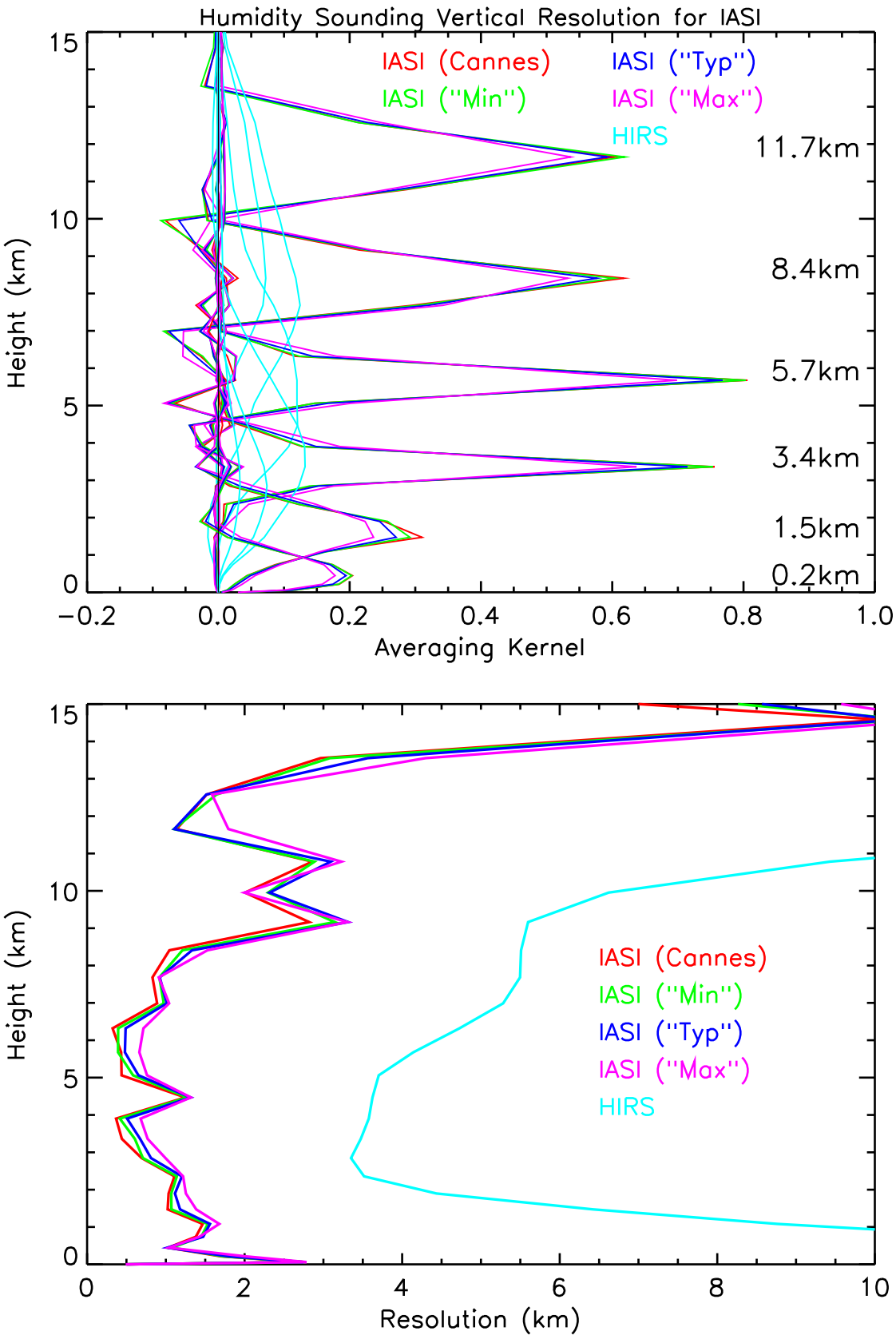

Fig. 9a. (Top) Selected averaging kernels for the retrieval of humidity using all available channels. The heights associated with each averaging kernel is indicated. Fig. 9b. (Bottom) Backus-Gilbert widths of the averaging kernels above as a function of height.

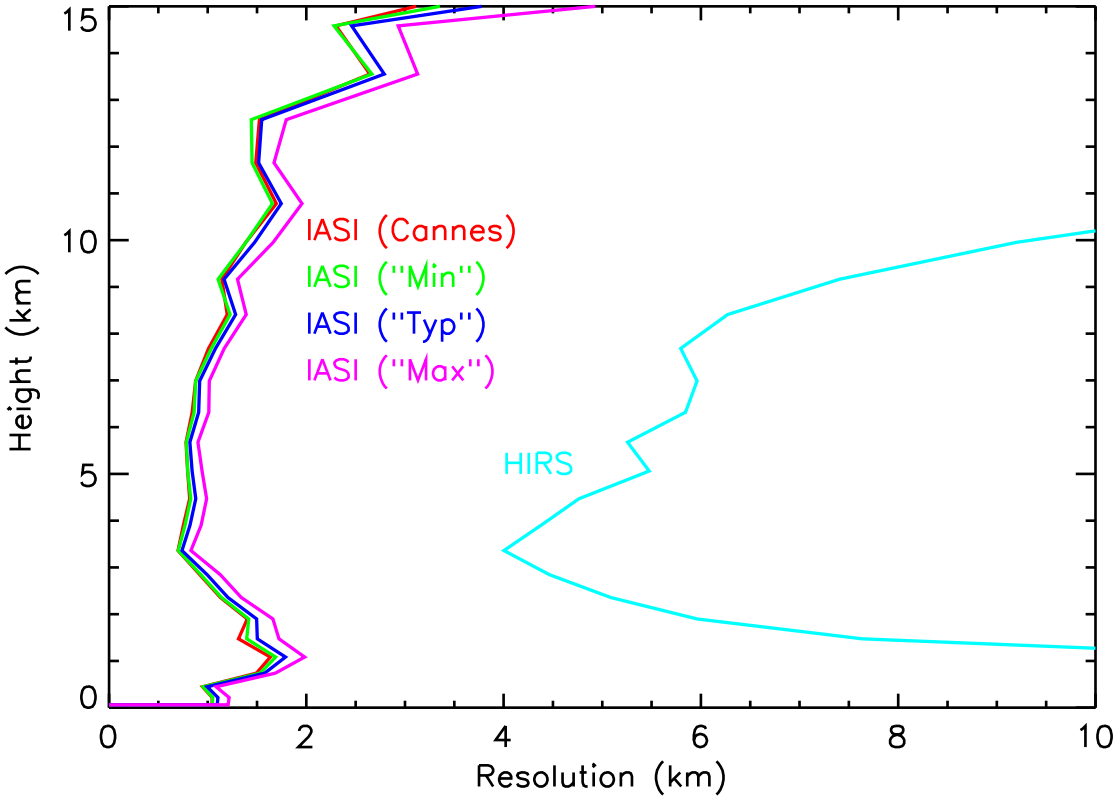

Fig. 9c. Vertical resolution of humidity retrievals defined in terms of effective data density.

Conclusion.

The three questions posed in the introduction thus may be answered as follows:

With the expected background error covariances, IASI will certainly meet the 1km-1K requirement if one takes the definition used by the AIRS project. If one chooses averaging kernel width (as defined in Eqn. 6) as the definition of 1km resolution, IASI is close (i.e., ~2km) in the optimal estimation case.

For humidity, the vertical resolution requirement is met in terms of the error on the retrieval of relative humidity. However, the absolute retrieval accuracy seems to fall somewhat short of 10%. The vertical resolution implied by the averaging kernal widths is close to 1km.

In all cases, IASI is a vast improvement over HIRS in both measurement accuracy and vertical resolution. Indeed, when vertical resolution is expressed in degrees of freedom, the improvement is by a factor of five.

On the final point, while it is, of course, best not to degrade the IASI noise performance in line with the CNES scenarios if possible, it will not significantly affect IASI's greatly improved performance compared to current satellite instruments.

References.

Backus, G.E. and J.F. Gilbert (1970). Uniqueness in the inversion of inaccurate gross Earth data. *Philos. Trans. R. Soc. London, Ser. A*, **266**, 123–192.

Diebel, D., F. Cayla and T. Phulpin (1996). *IASI Mission Rationale and Requirements. EUMETSAT/CNES Technical Report IA-SM-0000-10-CNE/EUM. Issue 4b.*

Eyre, J.R. (1987). On systematic errors in satellite sounding products and their climatological mean values. *Q.J.R. Meteorol. Soc.*, **113**, 279–292.

Eyre, J.R. (1998). The effects of nonlinearity on analysis and retrieval errors. *In Preparation.*

Ide, K., P. Courtier, M. Ghil and A.C. Lorenc (1997). Unified notation for data assimilation: Operational, sequential and variational. *J. Met. Soc. Japan*, **75**, 181–189.

Menke, W. (1984). *Geophysical data analysis: discrete inverse theory.* Academic Press, San Diego CA, USA.

Prunet, P., J.-N. Thépaut and V. Cassé (1998). The information content of clear sky IASI radiances and their potential for numerical weather prediction. *Q.J.R. Meteorol. Soc.,* **124,** 211–241.

Purser, R.J. and H.-L. Huang (1993). Estimating effective data density in a satellite retrieval or an objective analysis. *J. Appl. Meteor.,* 1092–1107.

Rabier, F., E. Klinker, P. Courtier and A. Hollingsworth (1996). Sensitivity of forecast errors to initial conditions. *Q.J.R. Meteorol. Soc.,* **122,** 121–150.

Rodgers, C.D. (1976). Retrieval of atmospheric temperature and composition from remote measurements of thermal radiation. *R. Geophys. Space Phys.*, **14**, 609–624.

Rodgers, C.D. (1990). Characterisation and error analysis of profiles retrieved from remote sounding measurements. *J. Geophys. Res.*, **95**, 5587–5595.

Rodgers, C.D. (1996). Information content and optimisation of high spectral resolution measurements. *SPIE*, **2830**, *Optical spectroscopic techniques and instrumentation for atmospheric and space research II,* Paul B. Hays and Jinxue Wang, eds., pp136–147.

Appendix A. The Discrete Version of the Backus-Gilbert Spread.

In the continuous case, the averaging kernel, $R^{\rm cont}(z_i, z_j)$, relates the true atmospheric state, $x(z_j)$, at height z_j, to the retrieved state, $\hat{x}(z_i)$, at height z_i via the equation

$$\hat{x}(z_i) = \int R^{\rm cont}(z_i, z_j) x(z_j) dz_j \qquad (A1)$$

$$\simeq \sum_j R^{\rm cont}(z_i, z_j) x_j \Delta z_j \qquad (A2)$$

where x_j is the true state at level j averaged over the height interval Δz_j and it is assumed that the background state is zero for clarity.

In the discrete case, the retrieved state, $\hat{x}_i$, for layer i is related to the "true" states, x_j, at each layer j by the averaging kernel, $\mathbf{R}^{\rm disc}$, via the relation

$$\hat{x}_i = \sum_j R_{ij}^{\rm disc} x_j. \qquad (A3)$$

Comparing Equations A2 and A3, one sees that

$$R_{ij}^{\rm disc} = R^{\rm cont}(z_i, z_j)\Delta z_j \qquad (A4)$$

i.e., the discrete resolution matrix has a factor Δz_i built into it relative to the continuous version (i.e., $R^{\rm cont}$ is a density).

The Backus-Gilbert spread is defined in, for example, Rodgers (1976) as

$$S(z_i) = 12\frac{\int (R^{\rm cont})^2(z_i, z_j)(z_j - z_i)^2 dz_j}{\left[\int R^{\rm cont}(z_i, z_j)dz_j\right]^2} \qquad (A5)$$

On discretising, the denominator of (A5) becomes $[\sum_j R_{ij}^{\rm disc}]^2$ while the numerator is

$$12\sum_j \left(R_{ij}^{\rm disc}/\Delta z_j\right)^2 (z_j - z_i)^2 \Delta z_j = 12\sum_j \left(R_{ij}^{\rm disc}\right)^2 (z_j - z_i)^2/\Delta z_j$$

Thus,

$$S(z_i) = 12\frac{\sum_j R_{ij}^{\rm disc}(z_j - z_i)^2/\Delta z_j}{[\sum_j R_{ij}^{\rm disc}]^2} \qquad (A6)$$

which is the form used in this study.

The Δz_j term in the last equation causes problems when Δz_j is zero. For atmospheric layers with zero thickness $R_{ij}^{\rm disc}$ should also be zero and (so long as Δz_j is set to a small positive value to avoid calculating 0/0) the expression is still valid. However, for the skin temperature one must remember that even in the continuous case the skin corresponds to a discrete "layer" and thus Equation (A1) becomes

$$\hat{x}(z_{\rm skin}) = \int R^{\rm cont}(z_i, z_j)\delta(z_j - z_{\rm skin})x(z_j)dz_j \qquad (A7)$$

$$= R^{\rm cont}(z_i, z_{\rm skin})x(z_{\rm skin}) \qquad (A8)$$

i.e., $\Delta z_j = 1$ in Equations (A4) and (A6).

Appendix B. Interpolation of Error Covariance Matrices.

The calculations in this document were done on the new 43-level scheme used at ECMWF. Apart from the obvious consideration that the IASI fastmodel has been produced for these levels by Marco Matricardi (ECMWF), this scheme has the advantage of having much finer pressure intervals in the lower layers of the atmosphere which reduces problems with the sub-sampling of the averaging kernels that was found when the current UKMO 40 level scheme was used.

However, at present no background error covariance matrices have been produced on the new 43 level scheme. It is thus necessary to somehow interpolate a 40 level matrix onto the new pressures. This has been done following a suggestion by B. Barwell (UKMO) where the eigenvectors of the original 40 level matrix, $\mathbf{B_{40}}$, are interpolated in log(pressure) onto the new 43 level grid. Taking the eigenvectors of $\mathbf{B_{40}}$ allows one to treat the matrix in terms of the variances (eigenvalues) of independent error patterns (the eigenvectors) and thus eliminates the need to consider covariances explicitly.

The resulting matrix of eigenvectors (plus three additional columns of zeroes), $\mathbf{X}$, and a diagonal matrix, $\mathbf{\Lambda}$, with the diagonal elements being the eigenvalues of $\mathbf{B_{40}}$ plus three zeros can thus be combined to form an intermediate 43-level error covariance matrix, $\mathbf{B_{43}^{tmp}}$, thus:

$$\mathbf{B_{43}^{tmp}} = \mathbf{X \Lambda X^T} \qquad (B1)$$

where the superscript $^{\mathbf{T}}$ denotes matrix transposition.

The interpolated eigenvectors, $\mathbf{X}$, are not necessarily orthogonal and hence are not the true eigenvectors of $\mathbf{B_{43}^{tmp}}$. Therefore, while $\mathbf{B_{43}^{tmp}}$ is a good approximation to $\mathbf{B_{40}}$ on 43 levels (and is guaranteed to be symmetric), it is not in general positive definite. This is fixed by manipulating the eigenvalues and eigenvectors of the new matrix.

In general, the eigenvalues of $\mathbf{B_{43}^{tmp}}$ can be sorted into a set of smoothly decreasing values but the last few values are often negative or very small and result in the matrix being ill-conditioned*. These small eigenvalues would imply that the atmospheric structures corresponding to their associated values are extremely well known *a priori* (negative values have no physical meaning whatsoever). These eigenvalues are thus set to values that would be expected from the trend in the larger eigenvalues and a final interpolated 43-level matrix, $\mathbf{B_{43}}$, is calculated using the form of Equation B1. Visual inspection of $\mathbf{B_{43}}$, its correlation structures and its diagonal elements (variances) implies good agreement with the original matrix $\mathbf{B_{40}}$.

* This is also often the case when an error covariance matrix is stored with not sufficient numerical precision.